Bioorganic Chemistry 100 (2020) 103906

Contents lists available at ScienceDirect

Bioorganic Chemistry

journal homepage: www.elsevier.com/locate/bioorg

# Synthesis and characterization of new 4*H*-chromene-3-carboxylates ensuring potent elastase inhibition activity along with their molecular docking and chemoinformatics properties

Nilam C. Dige[a,1], Prasad G. Mahajan[b,1], Hussain Raza[a], Mubashir Hassan[c], Balasaheb D. Vanjare[b], Hansol Hong[a], Ki Hwan Lee[b], Jalifah latip[d,*], Sung-Yum Seo[a,*]

[a] Department of Biological Sciences, Kongju National University, Gongju, Chungnam 32588, Republic of Korea
[b] Department of Chemistry, Kongju National University, Gongju, Chungnam 32588, Republic of Korea
[c] Institute of Molecular Biology and Biotechnology, The University of Lahore, Defence road, Lahore 54590, Pakistan
[d] School of Chemical Sciences and Food Technology, Faculty of Science and Technology, Universiti Kebangsaan Malaysia (UKM), 43600 Bangi, Selangor, Malaysia

ARTICLE INFO

*Keywords:*
Multicomponent synthesis
4*H*-chromene-3-carboxylate
Elastase Inhibitor
Lipinski's rule
Molecular docking

ABSTRACT

A new series of 4*H*-chromene-3-carboxylate derivatives were synthesized using multicomponent reaction of salicylaldehyde, ethyl acetoacetate and dimedone in ethanol with $K_3PO_4$ as a catalyst at 80 °C. The structures of all newly synthesized compounds were confirmed by spectral techniques *viz.* IR, $^1$H NMR, $^{13}$C NMR, and LCMS analysis. The newly synthesized compounds **4a to 4j** were screened against elastase enzyme. Interestingly, all these compounds found to be potent elastase inhibitors with much lower $IC_{50}$ value. The compound 4b was found to be most potent elastase inhibitor ($IC_{50}$ = 0.41 ± 0.01 μM) amongst the synthesized series against standard Oleanolic Acid ($IC_{50}$ value = 13.45 ± 0.0 μM). The Kinetics mechanism for compound **4b** was analyzed by Lineweaver-Burk plots which revealed that compound inhibited elastase competitively by forming an enzyme-inhibitor complex. Along with this, all the synthesized compounds **(4a – 4j)** exhibits excellent DPPH free radical scavenging ability. The inhibition constant $K_i$ for compound **4b** was found to be 0.6 μM. The computational study was comprehensible with the experimental results with good docking energy values (Kcal/mol). Therefore, these molecules can be considered as promising medicinal scaffolds for the treatment of skin-related maladies.

## 1. Introduction

In the development of modern organic chemistry, heterocyclic compounds play a significant role. With its origins rooted in organic synthesis and medicinal chemistry, heterocyclic compounds present themselves as a fundamental division of organic chemistry [1]. Chromenes are one of the major classes of naturally occurring heterocyclic compounds. They found in a large number of natural products and possess a wide range of biological activities [2]. Out of them functionalized 4*H*-chromenes have received considerable attention in recent years for their excellent biological properties such as anticoagulant [3], anticancer [4–7], spasmolytic and anti-anaphylactic [8–10], antimicrobial [11–13], antioxidant [14], and antimalarial [15] activities. Along with this, they have a role in pigments [16] and photoactive materials and are utilized as potential biodegradable agrochemicals [17]. This moiety also occurs in various natural products [18]. Several procedures for the preparation of 4*H*-chromenes with various starting materials have been reported in recent years [19].

Elastin is the protein widely distributed in the vertebrate tissues of human beings especially abundant in ligaments, lungs and skin. It is being hydrolyzed or cleaved by elastase enzyme belonging to the class of serine proteases [20]. It is also the key enzyme which attacks the all major matrix protein of connective tissue [21]. Skin aging is a naturally occurring process due to more exposure of skin by chronic ultra violet radiation. The continuous exposure of ultra violet radiations causes the formation of reactive oxygen species and lipid peroxides results into physical changes in the connective tissues and skin [22]. It leads to the loss of skin elasticity which can ultimately become the reason of wrinkle formation, brown spots, skin cancer, uneven pigmentation, leathery appearance, solar elastosis, laxity and melanoma [23–25].

* Corresponding authors.
*E-mail addresses:* jalifah@ukm.edu.my (J. latip), dnalove@kongju.ac.kr (S.-Y. Seo).
[1] these authors contributed equally for this research work.

https://doi.org/10.1016/j.bioorg.2020.103906
Received 4 February 2020; Received in revised form 8 April 2020; Accepted 30 April 2020
Available online 11 May 2020
0045-2068/ 

Elastase is the major responsible enzyme for wrinkle formation and dehydration on the skin [26]. It also causes delayed wound healings, increased inflammation progress and tissue permeability.

Recently, some medicinal plant's extracts have been reported as elastase inhibiting cosmeceuticals [27,28]. Along with this, some synthesized compounds, such as safranal [29], aryl and heteroaryl oxime ester derivatives [30], substituted perhalo-2-nitrobuta-1,3-dienes [31], and thiazol-2-(3H)-ones [32] have been reported as elastase inhibitors, but still the need for the development of superior and novel inhibitors is demanded. As per our continuation in synthesis of chromene compounds [33,34] and experience of previous efforts in enzyme inhibitory potential [35,36], we focus our attention towards design and synthesis of 4*H* chromene compounds which could be potent inhibitors against elastase activity.

## 2. Result and Discussion:

### 2.1. Chemistry:

In the beginning, we design and synthesize new 4*H*-chromene-3-carboxylates using multicomponent reaction of salicylaldehyde (1) (1 mmol), ethyl acetoacetate (2) (1 mmol) and dimedone (**3**) (1 mmol) in ethanol (Scheme 1). Favorably, the reaction proceeds well and resulting into the expected 4*H*-chromene-3-carboxylate product which was further confirmed by spectral techniques such as IR, $^{1}H$ & $^{13}C$ NMR and LCMS. The reaction of salicylaldehyde, ethyl acetoacetate and dimedone was chosen as a model reaction.

Initially, we tried to carry the model reaction without catalyst in ethanol at reflux condition (**Entry 1,** Table 1). But the reaction did not proceed well and results into very low yield of product. After that screening of various catalysts ($K_2CO_3$, $K_3PO_4$, $NH_4OAC$, DABCO and $NaHCO_3$) was done with model reaction using 30 mol% of each catalyst (**Entries 2 – 7,** Table 1). We found that out of all catalysts screened, $K_3PO_4$ drag the desired reaction with higher yield in less reaction time (**Entry 3,** Table 1). Therefore, we perform the screening of catalytic amount of $K_3PO_4$ for model reaction (**Entries 8 – 10,** Table 1). From Table 1, we can conclude that the 20 mol % of $K_3PO_4$ **(Entry 9,** Table 1**)** was found to be the enough and good catalytic amount for the proposed transformation. Therefore, the final optimized reaction conditions for present protocol are 20 mol % of $K_3PO_4$ in ethanol at 80 °C.

With this optimized reaction conditions in hand, such as 20 mol % of $K_3PO_4$ in ethanol at 80 °C, the generality of protocol was assessed using variety of substituted salicylaldehydes with electron donating and withdrawing group in its structure (Table 2). All reactions proceeds well in result of expected products with good to excellent yield. The products containing electron withdrawing group (**Entries 2 – 6,** Table 2) in its structure shows higher practical yield and short reaction time than the compounds containing electron donating group (**Entries 7 – 10,** Table 2). All the synthesized compounds were characterized with spectral techniques *viz.*, IR, NMR and LCMS. Pleasingly, the spectral data of synthesized compounds is in accordance with their expected structure. After successful synthesis and its characterization, all the synthesized compounds (**4a-4j**) were subjected to screen for their elastase activity. Satisfyingly, all synthesized compounds (**4a-4j**) exhibits good elastase inhibitory activity which was further supported by *in silico* analysis.

**Table 1**
Screening of catalyst.

| Entry | Catalyst | mol % | Time in min | Yield % |
|---|---|---|---|---|
| 1 | – | – | 180 | 32 |
| 2 | $K_2CO_3$ | 30 | 140 | 74 |
| 3 | $K_3PO_4$ | 30 | 125 | 85 |
| 4 | $NH_4OAC$ | 30 | 140 | 78 |
| 6 | DABCO | 30 | 150 | 77 |
| 7 | $NaHCO_3$ | 30 | 145 | 71 |
| 8 | $K_3PO_4$ | 10 | 130 | 82 |
| **9** | **$K_3PO_4$** | **20** | **120** | **87** |
| 10 | $K_3PO_4$ | 40 | 125 | 84 |

**Reaction conditions:** salicylaldehyde (1 mmol), Ethyl Acetoacetate (1 mmol), Dimedone (1 mmol), Solvent: Ethanol (10 mL), Temperature: 80 ℃

### 2.2. Biology:

#### 2.2.1. Elastase inhibition and structure activity relationship:

All newly synthesized compounds (**4a-4j**) were scrutinized for their inhibitory potentials against elastase enzyme. The results were outlined in Table 3. Most of the compounds exhibits potent inhibitory activity against elastase as evident from their much lower $IC_{50}$ values ($IC_{50}$ value = 0.41 ± 0.01 to 8.71 ± 0.66) as compared to standard oleanolic acid ($IC_{50}$ value = 13.45 ± 0.01 μM). All compounds revealed much lower $IC_{50}$ values than the standard oleanolic acid which signifies their potency for elastase inhibition.

The structure activity relationship (SAR) was predicted by the presence of substituent group on aryl ring, as it is the only variable part and remaining all other parts are similar in all molecules. The presence of electron withdrawing group on aromatic ring shows better activity than the compound containing electron donating group. Compound **4b** having Bromo substituent in its structure shows lowest $IC_{50}$ value ($IC_{50}$ = 0.41 ± 0.01 uM) as compared to standard oleanolic acid ($IC_{50}$ = 13.45 ± 0.01 μM). It means compound **4b** shows better elastase activity than the standard oleanolic acid. Along with this compounds **4c, 4d 4e** and **4f** ($IC_{50}$ = 7.64 ± 0.42, 7.66 ± 0.77, 3.66 ± 0.55 and 7.23 ± 0.64 uM) also contains electron withdrawing group in its structure possesses lower $IC_{50}$ value than the standard. Compound **4g – 4j** contains electron donating group in its structure. Here compound **4g** exceptionally shows lower $IC_{50}$ value **($IC_{50}$** = 0.99 ± 0.08 μM**)** than electron withdrawing group containing compounds except **4b** ($IC_{50}$ = 0.41 ± 0.01 uM). Compounds **4h, 4i** and **4j** ($IC_{50}$ = 8.71 ± 0.66, 11.38 ± 0.99 and 7.83 ± 0.77 uM)

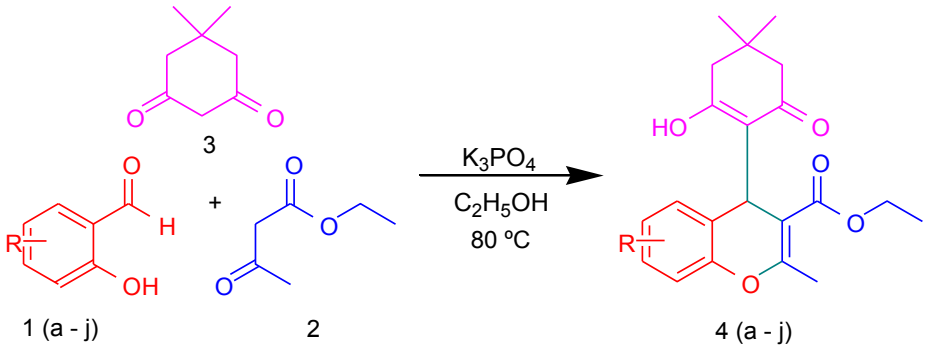


**Scheme 1.** Multicomponent Synthesis of 4*H*-chromene-3-carboxylates.

**Table 2**
Library of newly synthesized 4*H*-chromene-3-carboxylates.

| Entry | Code | Structure of compound | Time in min | Yield % |
|---|---|---|---|---|
| 1 | **4a** | 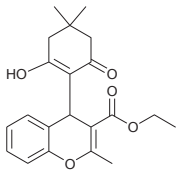 | 120 | 87 |
| 2 | **4b** | 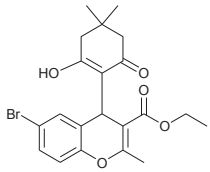 | 100 | 87 |
| 3 | **4c** | 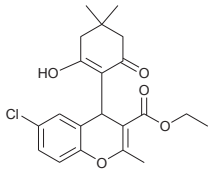 | 110 | 88 |
| 4 | **4d** | 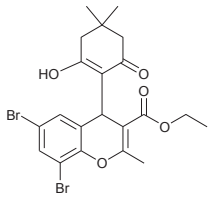 | 95 | 88 |
| 5 | **4e** | 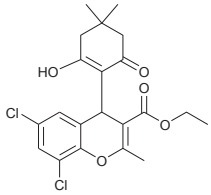 | 100 | 89 |
| 6 | **4f** | 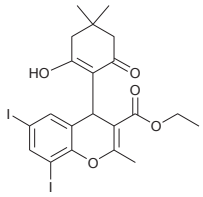 | 115 | 81 |
| 7 | **4g** | 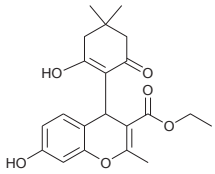 | 125 | 78 |
| 8 | **4h** | 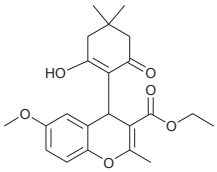 | 130 | 76 |
| 9 | **4i** | 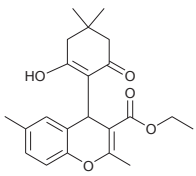 | 120 | 77 |

**Table 2** (*continued*)

| Entry | Code | Structure of compound | Time in min | Yield % |
|---|---|---|---|---|
| 10 | **4j** | 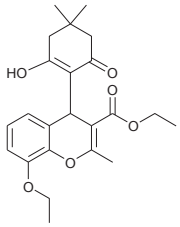 | 125 | 79 |

**Reaction conditions:** Respective salicylaldehyde (1 mmol), Ethyl Acetoacetate (1 mmol), Dimedone (1 mmol), Catalyst: 20 mol % $K_3PO_4$, Solvent: Ethanol (10 mL), Temperature: 80 °C

**Table 3**
Elastase (Elastase from porcine pancreas) inhibitory activity of **4a-4j** derivatives.

| Compound | Elastase $IC_{50}$ ± SEM (uM) |
|---|---|
| 4a | 9.86 ± 0.89 |
| **4b** | **0.41 ± 0.01** |
| 4c | 7.64 ± 0.42 |
| 4d | 7.66 ± 0.77 |
| 4e | 3.66 ± 0.55 |
| 4f | 7.23 ± 0.64 |
| 4g | 0.99 ± 0.08 |
| 4h | 8.71 ± 0.66 |
| 4i | 11.38 ± 0.99 |
| 4j | 7.83 ± 0.77 |
| Oleanolic Acid | 13.45 ± 0.01 |

SEM = Standard error of the mean; values are expressed in mean ± SEM.

shows comparatively higher $IC_{50}$ value than compound **4c, 4e** and **4f** but lower than the standard oleanolic acid ($IC_{50}$ = 13.45 ± 0.01 μM). Amongst the all synthesized and screened compounds, **4b** found to be more potent against the elastase inhibition. Therefore, it can be concluded that all 4*H*-chromene-3-carboxylate moiety bearing electron withdrawing groups on its structure possibly interacts more with the enzyme.

### 2.2.2. Kinetic Mechanism:

The inhibition kinetic study was performed to understand the inhibitory mode of synthetic compounds against elastase. Based upon $IC_{50}$ results, the most potent compound **4b** was selected to determine their inhibition type and inhibition constant. The kinetic study of the enzyme involves the examination of Lineweaver-Burk plot of 1/V versus substrate *N*-succinyl-Ala-Ala-Ala-*p*-nitroanilide 1/[S] in the presence of different inhibitor concentrations resulted into a series of straight lines (Fig. 1**A**). The Lineweaver-Burk plot of compound **4b** showed that $V_{max}$ remains same without significantly affecting the slopes. Whereas, $K_m$ increases with increasing concentration and $V_{max}$ remains the same with insignificant difference. This behavior indicates that compound **4b** inhibits the enzymes in competitive manner (Fig. 1**A**). The enzyme Inhibition dissociation constant (*Ki*) was determined by plotting slope against inhibitor concentration of **4b** (Fig. 1**B**), which was found to be 0.6 μM.

### 2.2.3. Free radical scavenging:

All the synthesized 4*H*-chromene-3-carboxylates **(4a-4j)** were assessed for their DPPH free radical scavenging ability at the concentration of (100 μg/mL). The results were presented in Fig. 2. In comparison with standard vitamin C, all synthesized 4*H*-chromene-3-carboxylate compounds **(4a-4j)** shows excellent free radical scavenging activity.

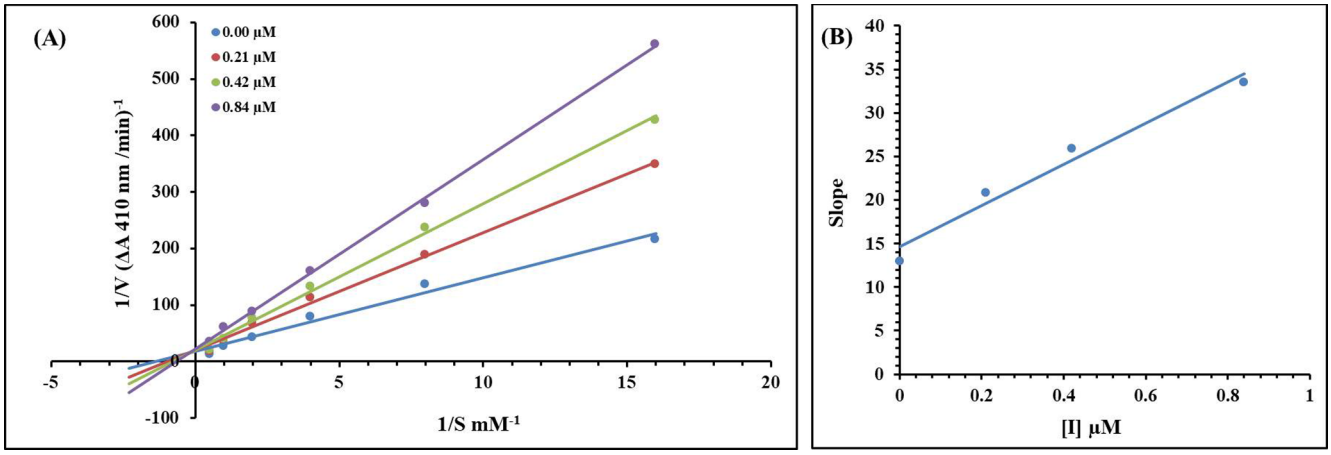


**Fig. 1.** Lineweaver–Burk plot for inhibition of elastase from porcine pancreas in the presence of Compound **4b**. **(A)** Concentrations of **4b** were 0.00, 0.21, 0.42 and 0.84 µM, Substrate *N*-succinyl-Ala-Ala-Ala-*p*-nitroanilide concentrations were 2, 1, 0.5, 0.25, 0.125 and 0.0625 mM, respectively. **(B)** The insets represent the plot of the slope versus inhibitor **4b** concentrations to determine inhibition constant.

*2.2.4. Chemoinformatics properties of newly synthesized 4H-chromene-3-carboxylates (4a −4j):*

The basic Chemoinformatics properties of all synthesized compounds (**4a-4j**) were predicted by using computational tools. The predicted properties like molecular weight (Mol. Wt. g/mol), number of hydrogen bond acceptor and donors (No. HBA/HBD), LogP, polar surface area (PSA, $A^2$) and molecular volume (Mol. Vol, $A^3$) were shown in Table 4. The Mol. Wt (g/mol) and number of HBA and HBD in all synthesized compounds were found to be comparable with the standard values < 500 (g/mol) Mol. Wt. and < 10 HBA with < 5 HBD, respectively. Though **4f** exhibited greater Mol. Wt. (609 g/mol) compared to standard results, it follows Lipinski's rule. It is well known that the exceed values of HBA and HBD results in poor permeation [37,38]. The hydrogen-bonding capacity has been considered as significant parameter for drug permeability. Our results justified that the all synthesized compounds (**4a-4j**) possess < 10 HBA and < 5 HBD values which were comparable with standard values. Additionally, the analyzed data for synthesized compounds showed that PSA is very helpful parameter for drug absorption prediction in drug discovery [37,38]. The reported study showed that molecules with poor absorption are more likely to be observed to violate the Lipinski's rule. Multiple examples are available for RO5 violation amongst the existing drugs [39–40].

**Table 4**
Predicted Chemoinformatics properties of synthesized compounds **4a −4j.**

| Compounds | Mol. Wt. (g/mol) | No. HBA | No. HBD | Mol. Log*P* | Mol PSA ($A^2$) | Mol. Vol ($A^3$) |
|---|---|---|---|---|---|---|
| **4a** | 358 | 5 | 1 | 2.9 | 57 | 452 |
| **4b** | 434 | 5 | 1 | 5.1 | 56 | 440 |
| **4c** | 390 | 5 | 1 | 5.0 | 56 | 435 |
| **4d** | 511 | 5 | 1 | 5.8 | 56 | 460 |
| **4e** | 424 | 5 | 1 | 5.6 | 56 | 450 |
| **4f** | 609 | 5 | 1 | 5.7 | 56 | 477 |
| **4g** | 372 | 6 | 2 | 4.0 | 74 | 428 |
| **4h** | 386 | 6 | 1 | 4.4 | 64 | 450 |
| **4i** | 370 | 5 | 1 | 4.7 | 56 | 439 |
| **4j** | 400 | 6 | 1 | 4.7 | 63 | 467 |

*2.2.5. Docking Analysis:*

*2.2.5.1. Structural evaluation of target protein.* Porcine pancreatic elastase consists of 240 amino acids having calcium atom embedded

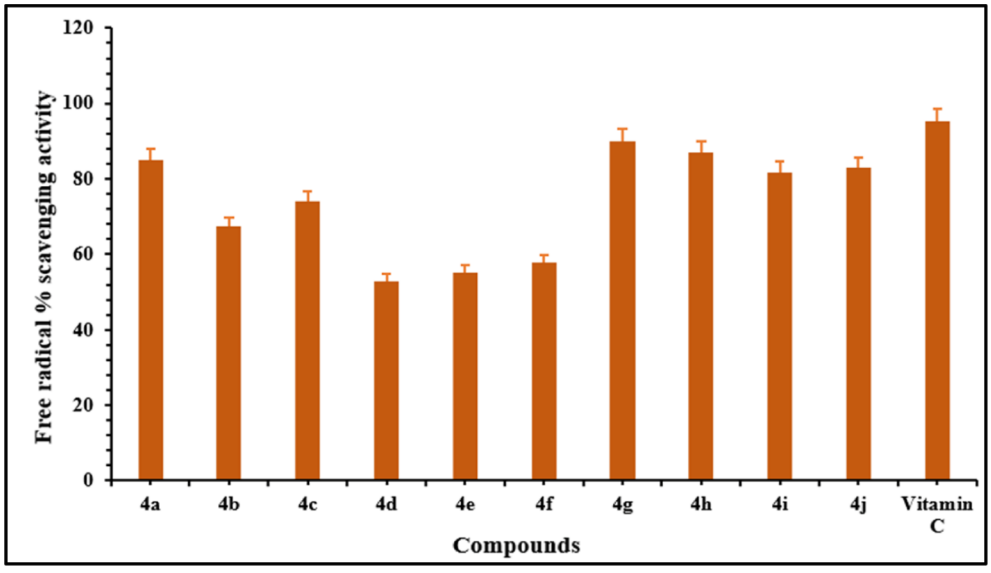


**Fig. 2.** Free radical scavenging activity of synthesized compounds. Values were represented as mean ± SEM. All compounds concentrations were 100 µg/mL.

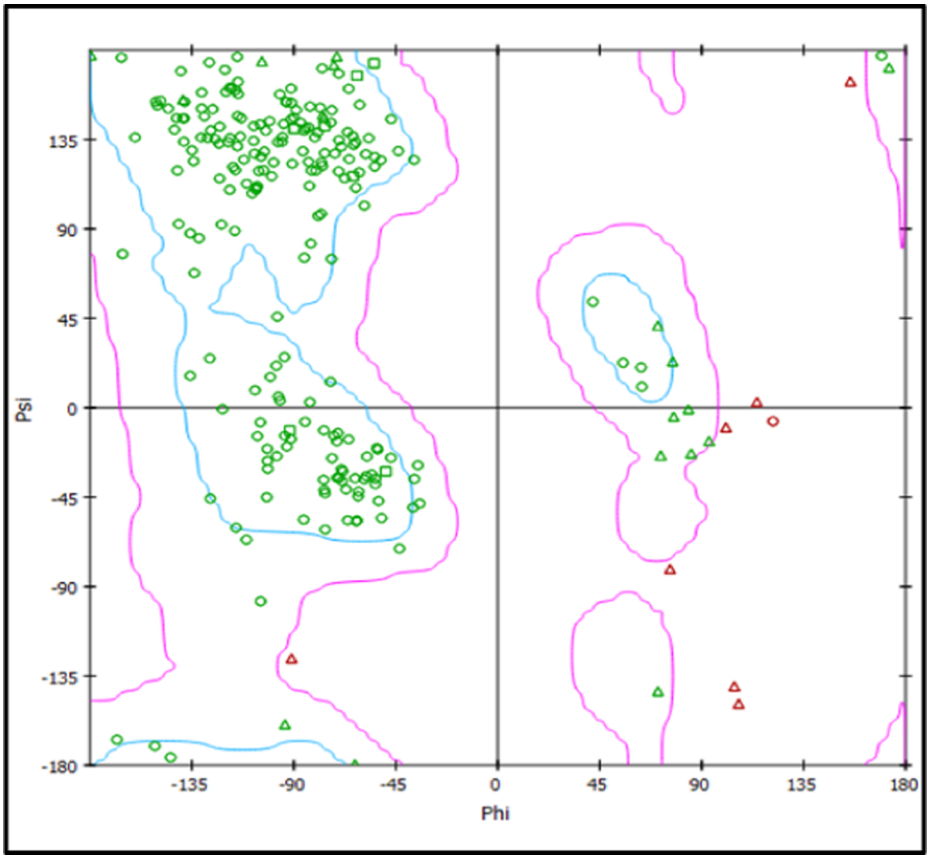


**Fig. 3.** Ramachandran plot of porcine pancreatic elastase.

in the protein structure. The x-ray diffraction study showed its resolution: 1.8 Å having unit cell coordinates a = 52.530, b = 57.470 and c = 75.260 with angles α = 90.00, β = 90.00 and γ = 90.00, respectively. The Ramachandran graph values also showed 88.70% of residues were present in favored region while 98.70% residues were lie in allowed region (Fig. 3).

*2.2.5.2. Docking energy analyses of synthesized compounds:*. To predict the best fitted conformational position of synthesized compounds (**4a-4j**) within the active region of targeted protein. The predicted docked complexes were evaluated on the basis of minimum energy values (kcal/mol) and interaction pattern. Docking results illustrates that all compounds showed good energy values ranging from −7.5 to −8.5 Kcal/mol. The docking energy values of all the docking complexes were calculated by using equation (1).

$$\Delta G\,\text{binding} = \Delta G\text{gauss} + \Delta G\text{repulsion} + \Delta G\text{hbond} + \Delta G\text{hydrophobic} + \Delta G\text{tors} \quad (1)$$

where, ΔGgauss: attractive term for dispersion of two gaussian functions, ΔGrepulsion: square of the distance if closer than a threshold value, ΔGhbond: ramp function - also used for interactions with metal ions, ΔGhydrophobic: ramp function, ΔGtors: proportional to the number of rotatable bonds.

Present docking results for synthesized compounds (**4a-4j**) indicates the energy value difference among all docking complexes were lower than standard error value (Fig. 4). Therefore, based on the basis of both *in vitro* and *in silico* docking energy results, **4b** is ranked as best ligand which shows good inhibitory potential against targeted enzyme as compared to all other derivatives.

*2.2.5.3. Binding pocket and ligand conformation*. The binding pocket

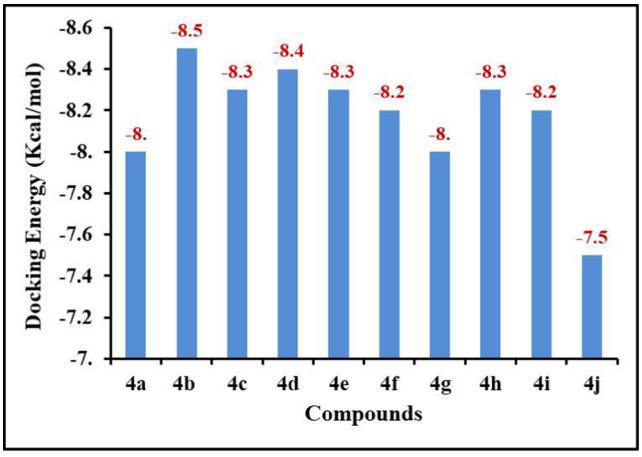


**Fig. 4.** Docking energy values of synthesized compounds.

analysis showed that compounds were confined in the active region of target protein (Fig. 5**A**). Results showed that compound **4b** binds in good conformation in the binding pocket of target protein. The methyl part (**$CH_3$**) showed their entrance inside the binding pocket, whereas halogen moiety was present at the opening region of target protein. This incorporation may results in suitable configuration and conformation to ligand to be fitted in the binding pocket of elastase (Fig. 5**B**).

*2.2.5.4. Hydrogen binding analysis*. The docked complexes were analyzed on the basis of hydrogen and hydrophobic bonding interactions. Based on *in-vitro* result compound **4b** was selected to check best conformational position inside active region of target protein. The compound **4b** forms two hydrogen bonds at two

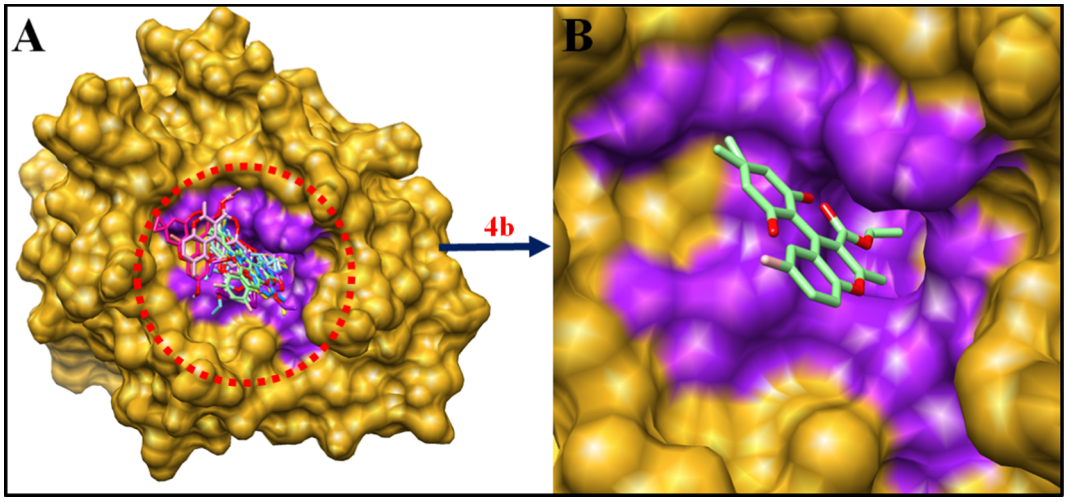


**Fig. 5.** Binding pocket of elastase **(A)** with embedded compound **4b** (**B**).

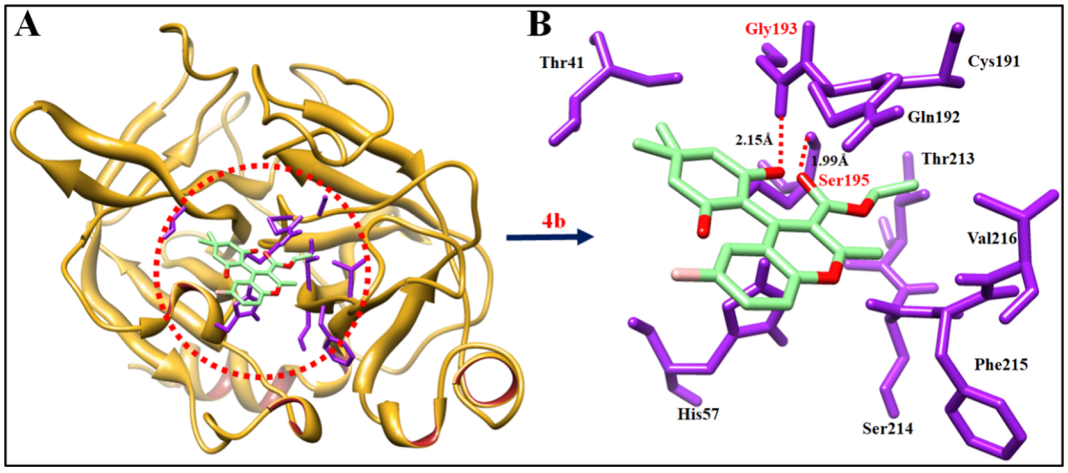


**Fig. 6.** Molecular docking interaction of **4b** against receptor molecule. **(A)** The general overview of docking depiction. The protein structure is represented in dark brown color in ribbon format while ligand is highlighted in cyan color. **(B)** The closer view of binding pocket interaction with best conformation position of ligand against target protein. The interacted amino acids are highlighted in purple color and red dotted lines with distance mentioned in angstrom (Å) are justified for hydrogen and bond distances.

different residues against target protein. The oxygen atoms of benzene ring form hydrogen bonds with Gly193 and Ser195 with bond length 2.15 and 1.99 Å, respectively. Literature data also ensured the importance of these residues in bonding with other elastase inhibitors which strengthen our docking results [40,41]. The docking depiction is mentioned in Fig. 6**A** and Fig. 6**B**.

## 3. Conclusion:

The successful multicomponent synthesis of 4*H*-chromene-3-carboxylates was performed using $K_3PO_4$ as catalyst in ethanol at 80 °C. The noteworthy features of this protocol are easy and simple workup procedure, high atom economy, excellent substrate scope, less reaction time and high yield of 4*H*-chromene-3-carboxylates. It is noteworthy that all synthesized compounds (**4a** −**4j**) possessing superior elastase inhibitor activity. Particularly, compound **4b** ($IC_{50}$ = 0.41 ± 0.01 μM) exhibits excellent activity as compared to standard Oleanolic Acid ($IC_{50}$ = 13.45 ± 0.01 μM). In addition, DPPH assay signposted excellent antioxidant properties for all the synthesized carboxylates. The *in silico* molecular docking investigation is in support of *in vitro* findings. Overall, from the results on biological activity and molecular docking studies of synthesized compounds **4a** − **4j**, it can be concluded that these compounds can be utilized as leading medicinal templates in molecular drug design for elastase inhibition and skin disorder.

## 4. Experimental:

### 4.1. Chemistry

#### 4.1.1. Materials and Method

Various substituted salicylaldehydes, Ethyl Acetoacetate, Dimedone and Potassium phosphate ($K_3PO_4$) were purchased from Sigma-Aldrich, Korea and used as received without further purification. Digimelt (SRS, USA) melting point apparatus was used to measure melting point of synthesized carboxylates. The formation of carboxlates (**4a-4j**) was confirmed by spectral techniques such as IR, NMR and LCMS Analysis. IR spectra were recorded on a Frontier IR Perkin–Elmer spectrophotometer. NMR spectra were recorded on a Bruker Avance III 600 MHz FT-NMR spectrometer in DMSO-$d_6$ using tetramethylsilane as an internal standard. The LCMS spectra were recorded on a Bruker MicroTof-Q spectrometer (Germany) coupled with Dionex Ultimate 3000/LC 09,115,047 (USA).

#### 4.1.2. General synthetic procedure for the synthesis of 4H-chromene-3-carboxylates (4a −4j)

The 50 mL of round bottom flask equipped with respective

substituted salicylaldehyde (1 mmol), ethyl acetoactate (1 mmol) and $K_3PO_4$ (20 mol%) in ethanol (10 mL). The reaction mixture was refluxed at 80 ℃ till formation of Knoevenagel adduct. Then an equivalent amount of dimedone (1 mmol) was added in it and the resultant reaction mixture was further refluxed at 80 ℃ till the completion of reaction. The progress of reaction was monitored using thin layer chromatography. After completion of reaction, the reaction mixture was cooled and ice water was added in it. The expected product was precipitated out which was separated just by simple filtration. The crude product was again recrystallized using hot methanol in order to recieve the product in its pure form. The formation of expected product was confirmed by spectral techniques such as IR, $^1$H & $^{13}$C NMR and LCMS analysis.

*4.1.2.1. Ethyl 4-(2-hydroxy-4,4-dimi8methyl-6-oxocyclohex-1-enyl)-2-methyl-4H-chromene-3-carboxylate (4a)*. Off White powder; M.P.: 208 ˚C; IR: 3175, 2968, 1726, 1641, 1592, 1520, 1362, 1260, 1232, 1189, 1082, 1008, 850, 756, 680 $cm^{-1}$; $^1$H NMR(600 MHz, DMSO-$d_6$): $\delta$ 10.36 (s, 1H, –OH), 7.08 – 7.11 (m, 1H), 6.92 – 6.99 (m, 3H), 5.05 (s, 1H), 2.52–2.55 (d, 2H, $J$ = 18H), 2.22 – 2.35 (q, 2H), 2.03 – 2.05 (d, 2H, $J$ = 18), 1.05 (S, 3H), 0.98 (S, 3H), 0.89 (S, 6H) ppm; $^{13}$C NMR (150 MHz, DMSO-$d_6$) : $\delta$ 169.20, 195.55, 165.16, 150.13, 128.86, 127.30, 126.11, 124.60, 115.78, 11.28, 50.93, 43.47, 41.17, 32.06, 29.63, 28.20, 26.73 ppm; LCMS (ESI): 355.1765 (M − 1) *m/z*.

*4.1.2.2. Ethyl 6-bromo-4-(2-hydroxy-4,4-dimethyl-6-oxocyclohex-1-enyl)-2-methyl-4H-chromene-3-carboxylate (4b)*. Cream color powder; M.P.: 225 ˚C; IR: 3118, 2961, 1733, 1614, 1474, 1364, 1250, 1180, 1136, 1079, 1039, 1011, 982, 969, 834, 820, 755, 658 $cm^{-1}$; $^1$H NMR (600 MHz, DMSO-$d_6$): $\delta$ 10.54 (s, 1H, –OH), 7.26 – 7.28 (m, 1H), 6.93 – 7.04 (m,2H), 5.03 (s, 1H), 2.58 (s, 2H), 2.23 – 2.34 (q, 2H), 2.02 – 2.05 (d, 2H, $J$ = 18), 1.04 (S, 3H), 0.97 (S, 3H), 0.89 (S, 6H) ppm; $^{13}$C NMR (150 MHz, DMSO-$d_6$) : $\delta$ 196.08, 195.40, 164.92, 158.43, 154.10, 149.45, 146.06, 137.04, 133.00, 131.04, 130.15, 128.78, 125.93, 120.54, 118.87, 118.20, 116.81, 115.90, 110.94, 50.85, 41.00, 32.06, 30.43, 29.56, 28.08, 26.64 ppm; LCMS (ESI): 435.0804 $M^+$ and 347.0784 (M + 2) *m/z*

*4.1.2.3. Ethyl 6-chloro-4-(2-hydroxy-4,4-dimethyl-6-oxocyclohex-1-enyl)-2-methyl-4H-chromene-3-carboxylate (4c)*. Light yellow powder; M.P.: 212 ˚C; IR: 2960, 1736, 1716, 1621, 1575, 1479, 1373, 1282, 1182, 1074, 1039, 1012, 933, 877, 836, 822 $cm^{-1}$; $^1$H NMR(600 MHz, DMSO-$d_6$): $\delta$ 10.56 (s, 1H, –OH), 7.14 – 7.16 (m, 1H), 7.99 – 7.00 (d, 1H, $J$ = 6 MHz), 6.90 – 6.91 (d, 1H, $J$ = 6 MHz), 5.04 (s, 1H), 2.53–2.59 (m, 2H), 2.23 – 2.35 (q, 2H), 2.03 – 2.05 (d, 2H, $J$ = 12 MHz), 1.05 (S, 3H), 0.97 (S, 3H), 0.90 (S, 6H) ppm; $^{13}$C NMR (150 MHz, DMSO-$d_6$) : $\delta$ 196.09, 164.90, 153.69, 149.00, 146.13, 134.28, 129.98, 128.32, 128.08, 128.00, 127.27, 118.61, 117.76, 110.86, 50.86, 41.01, 32.04, 29.60, 28.11, 26.64 ppm; LCMS (ESI): 391.1307(M + 1) *m/z*

*4.1.2.4. Ethyl 6,8-dibromo-4-(2-hydroxy-4,4-dimethyl-6-oxocyclohex-1-enyl)-2-methyl-4H-chromene-3-carboxylate (4d)*. Beige powder; M.P.: 231 ˚C; IR: 3175, 2960, 1747, 1667, 1646, 1598, 1563, 1449, 1373, 1313, 1246, 1206, 1181, 1149, 1038, 1011, 852, 764, 699 $cm^{-1}$; $^1$H NMR(600 MHz, DMSO-$d_6$): $\delta$ 10.71 (s, 1H, –OH), 8.22 – 8.25 (m, 1H), 7.62 – 7.63 (d, 1H, $J$ = 6 MHz), 7.01 – 7.02 (d, 1H, $J$ = 6 MHz), 5.06 (s, 1H), 2.55–2.60 (m, 2H), 2.25 – 2.27 (d, 2H, $J$ = 12 MHz), 2.03 – 2.06 (d, 2H, $J$ = 18 MHz), 1.06 (S, 3H), 0.97 (S, 3H), 0.89 (S, 6H) ppm; $^{13}$C NMR(150 MHz, DMSO-$d_6$) : $\delta$ 196.05, 195.09, 164.53, 157.76, 150.92, 146.54, 145.77, 138.84, 132.77, 132.65, 130.56, 130.14, 126.49, 121.53, 116.85, 115.93, 111.31, 110.73, 50.82, 40.80, 32.13, 30.37, 29.53, 28.07, 26.54 ppm; LCMS (ESI): 514.12 $M^+$ *m/z*

*4.1.2.5. Ethyl 6,8-dichloro-4-(2-hydroxy-4,4-dimethyl-6-oxocyclohex-1-enyl)-2-methyl-4H-chromene-3-carboxylate (4e)*. Off White powder; M.P.: 207 ˚C; IR: 3174, 2961, 1746, 1667, 1646, 1600, 1450, 1378, 1313, 1257, 1207, 1190, 1150, 1040, 1026, 1012, 886, 854, 764 $cm^{-1}$; $^1$H NMR(600 MHz, DMSO-$d_6$): $\delta$ 10.72 (s, 1H, –OH), 7.41 (s, 1H), 6.86 (s, 1H), 5.06 (s, 1H), 2.54–2.60 (m, 2H), 2.25 – 2.28 (d, 2H, $J$ = 18 MHz), 2.04 – 2.07 (d, 2H, $J$ = 18 MHz), 1.06 (S, 3H), 0.97 (S, 3H), 0.89 (S, 6H) ppm; $^{13}$C NMR(150 MHz, DMSO-$d_6$) : $\delta$ 197.26, 196.06, 164.63, 164.41, 145.13, 129.78, 127.91, 127.40, 127.01, 121.21, 111.18, 50.82, 40.79, 32.11, 32.04, 29.52, 29.03, 28.04, 26.54 ppm; LCMS (ESI): 425.0918 $M^+$ *m/z*

*4.1.2.6. Ethyl 4-(2-hydroxy-4,4-dimethyl-6-oxocyclohex-1-enyl)-6,8-diiodo-2-methyl-4H-chromene-3-carboxylate (4f)*. Beige powder; M.P.: 223 ˚C; IR: 3181, 2959, 2872, 1738, 1645, 1590, 1551, 1443, 1373, 1312, 1254, 1242, 1206, 1177, 1147, 1010, 980, 872, 854, 764, 694, 677 $cm^{-1}$; $^1$H NMR(600 MHz, DMSO-$d_6$): $\delta$ 10.64 (s, 1H, –OH), 7.85 (s, 1H), 7.18 (s, 1H), 5.01 (s, 1H), 2.56 – 2.59 (t, 2H, $J$ = 6 & 12 MHz), 2.35–2.38 (d, 2H, $J$ = 18 MHz), 2.24 – 2.27 (d, 2H, $J$ = 18 MHz), 2.02 – 2.05 (d, 2H, $J$ = 18 MHz), 1.06 (S, 3H), 0.97 (S, 3H), 0.89 (S, 6H) ppm; $^{13}$C NMR(150 MHz, DMSO-$d_6$) : $\delta$ 196.00, 164.79, 159.35, 154.14, 152.06, 149.60, 143.77, 137.26, 129.55, 126.10, 121.17, 111.56, 88.86, 86.82, 50.85, 40.87, 32.14, 30.43, 29.59, 28.06, 26.56 ppm; LCMS (ESI): 608.0570 $M^+$ *m/z*

*4.1.2.7. Ethyl 7-hydroxy-4-(2-hydroxy-4,4-dimethyl-6-oxocyclohex-1-enyl)-2-methyl-4H-chromene-3-carboxylate (4g)*. Light Brown powder; M.P.: 234 ˚C; IR: 3174, 2953, 2885, 1744, 1619, 1588, 1515, 1451, 1368, 1308, 1263, 1231, 1172, 1143, 1097, 1032, 1012, 973, 844, 814, 769, 662 $cm^{-1}$; $^1$H NMR(600 MHz, DMSO-$d_6$): $\delta$ 10.20 (s, 1H, –OH), 9.34 (s, 1H, –OH), 6.73 – 6.74 (d, 1H, $J$ = 6 MHz), 6.40 – 6.41 (d, 1H, $J$ = 6 MHz), 6.31 (s, 1H), 4.92 (s, 1H), 2.29 – 2.31(d, 2H, $J$ = 12 MHz), 2.20–2.22 (d, 2H, $J$ = 12 MHz), 2.00 – 2.02 (d, 2H, $J$ = 12 MHz), 1.03 (S, 3H), 0.97 (S, 3H), 0.89 (S, 6H) ppm; $^{13}$C NMR(150 MHz, DMSO-$d_6$) : $\delta$ 196.27, 195.62, 165.07, 156.57, 150.54, 129.23, 116.40, 112.24, 111.66, 102.35, 50.97, 43.55, 41.22, 32.02, 29.62, 28.21, 26.78 ppm; LCMS (ESI): 373.1644(M + 1) *m/z*

*4.1.2.8. Ethyl 4-(2-hydroxy-4,4-dimethyl-6-oxocyclohex-1-enyl)-6-methoxy-2-methyl-4H-chromene-3-carboxylate (4h)*. Light Beige powder; M.P.: 222 ˚C; IR: 3192, 2942, 1728, 1634, 1591, 1497, 1468, 1422, 1373, 1318, 1265, 1223, 1199, 1152, 1130, 1027, 1012, 855, 814, 746, 662 $cm^{-1}$; $^1$H NMR(600 MHz, DMSO-$d_6$): $\delta$ 10.32 (s, 1H, –OH), 6.88 – 6.89 (d, 1H, $J$ = 6 MHz), 6.67 – 6.69 (q, 1H), 6.46 (s, 1H), 5.02 (s, 1H), 3.63 (s, 3H), 2.50 – 2.53(d, 2H, $J$ = 18 MHz), 2.21–2.32 (q, 2H), 2.01 – 2.03 (d, 2H, $J$ = 12 MHz), 1.04 (S, 3H), 0.98 (S, 3H), 0.90 (S, 6H) ppm; $^{13}$C NMR(150 MHz, DMSO-$d_6$) : $\delta$ 196.15, 195.65, 165.33, 159.05, 156.28, 156.08, 149.62, 147.30, 144.30, 127.06, 125.12, 122.82, 119.06, 117.70, 116.54, 113.24, 112.79, 112.70, 110.51, 56.30, 55.66, 50.93, 41.22, 32.03, 30.48, 29.65, 28.13, 26.73 ppm;

*4.1.2.9. Ethyl 4-(2-hydroxy-4,4-dimethyl-6-oxocyclohex-1-enyl)-2,6-dimethyl-4H-chromene-3-carboxylate (4i)*. White powder; M.P.: 213 ˚C; IR: 3104, 2962, 2942, 1735, 1626, 1613, 1585, 1494, 1372, 1307, 1245, 1223, 1202, 1172, 1153, 1076, 1041, 1011, 934, 886, 818, 781, 657 $cm^{-1}$; $^1$H NMR(600 MHz, DMSO-$d_6$): $\delta$ 10.29 (s, 1H, –OH), 6.89 – 6.91 (q, 1H), 6.82 – 6.83 (d, 1H, $J$ = 6 MHz), 6.75 (s, 1H), 5.01 (s, 1H), 2.31 – 2.33 (d, 2H, $J$ = 12 MHz), 2.22–2.25 (d, 2H, $J$ = 18 MHz), 2.16 (s, 3H), 2.01 – 2.04 (d, 2H, $J$ = 18 MHz), 1.05 (S, 3H), 0.98 (S, 3H), 0.90 (S, 3H), 0.89 (s, 3H) ppm; $^{13}$C NMR(150 MHz, DMSO-$d_6$) : $\delta$ 196.18, 165.25, 148.15, 133.38, 128.98, 127.82, 125.78, 115.54, 111.15, 50.96, 43.50, 41.21, 32.04, 29.65, 28.13, 26.71, 20.81 ppm; LCMS (ESI): 369.2051(M − 1) *m/z*

*4.1.2.10. Ethyl 8-ethoxy-4-(2-hydroxy-4,4-dimethyl-6-oxocyclohex-1-enyl)-2-methyl-4H-chromene-3-carboxylate (4j)*. Light yellow powder; M.P.: 142 ˚C; IR: 2960, 2871, 2565, 1729, 1634, 1612, 1582, 1566,

1471, 1371, 1332, 1316, 1257, 1227, 1207, 1195, 1132, 1089, 1074, 1027, 886, 788, 760, 727 $cm^{-1}$; $^1H$ NMR(600 MHz, DMSO-$d_6$): $\delta$ 10.31 (s, 1H, –OH), 6.88 (t, 1H, $J$ = 12 MHz), 6.77 – 6.78 (d, 1H, $J$ = 6 MHz), 6.51 – 6.53 (d, 1H, $J$ = 12 MH), 5.03 (s, 1H), 4.03 – 4.05 (q, 2H), 2.56–2.59 (d, 1H, $J$ = 18 MH), 2.21 – 2.37 (q, 2H), 2.02 – 2.04 (d, 2H, $J$ = 12 MHz), 1.35 (t, 3H, $J$ = 6 &12 MHz), 1.05 (S, 3H), 0.99 (S, 3H), 0.89 (s, 6H) ppm; $^{13}C$ NMR(150 MHz, DMSO-$d_6$) : $\delta$ 196.23, 158.68, 147.73, 146.39, 139.86, 126.83, 125.32, 124.17, 122.12, 120.19, 117.88, 111.25, 65.06, 64.32, 56.50, 32.10, 30.43, 29.60, 28.12, 26.70, 19.01, 15.20 ppm; LCMS (ESI): 400.2220 $M^+$ $m/z$

### 4.2. Biology:

#### 4.2.1. In vitro Methodology:

*4.2.1.1. Elastase inhibition assay:*. The elastase (Elastase from porcine pancreas) inhibition activity was performed by following already reported method [42–45] with few modifications. In order to perform the inhibition of elastase activity, the amount of released *p*-nitroaniline, which was hydrolyzed from the substrate (*N*-succinyl-Ala-Ala-Ala-*p*-nitroanilide) by elastase, was determined by measuring the absorbance at 410 nm. In detail, 0.8 mM solution of *N*-succinyl-Ala-Ala-Ala-*p*-nitroanilide was prepared in a 0.2 M Tris-HCl buffer (pH 8.0) and this buffer (130 μL) was added to the test sample (10 μL) in a 96 well microplate. The microplate was pre-incubated for 10 min at 25 °C before an elastase (0.0375 Unit/mL) stock solution (10 μL) was added. After enzyme addition, the microplate was kept at 25 °C for 30 min, and the absorbance was measured at 410 nm using microplate reader (SpectraMax ABS, USA). $IC_{50}$ values were calculated by nonlinear regression using GraphPad Prism 5.0 (GraphPad, San Diego, CA USA). All experiments were carried out in triplicate. The elastase inhibition activities were calculated according to the following formula:

$$\text{Elastaseinhibitionactivity}(\%) = \frac{OD_{Control} - OD_{Sample}}{OD_{Control}} \times 100 \quad (2)$$

where, $OD_{control}$ and $OD_{sample}$ represents the optical densities in the absence and presence of sample, respectively. Oleanolic acid was used as the standard inhibitor for elastase.

*4.2.1.2. Kinetic analysis of inhibition of elastase:*. By following our reported method [46] Kinetic analysis was carried out to determine the mode of inhibition. The Compound **4b** was selected on the basis of most potent $IC_{50}$ values. Kinetic study was carried out by varying the concentration of *N*-succinyl-Ala-Ala-Ala-*p*-nitroanilide in the presence of different concentrations of compound **4b** (0.00, 0.21, 0.42 and 0.84 μM). Briefly the *N*-succinyl-Ala-Ala-Ala-*p*-nitroanilide concentration was changed from 2, 1, 0.5, 0.25, 0.125 and 0.0625 mM for its kinetics studies and remaining procedure was same for all kinetic studies as describes in elastase inhibition assay protocol. Maximal initial velocities were determined from initial linear portion of absorbance's up to 10 min after addition of enzyme at per minute interval. The inhibition type on the enzyme was evaluated by Lineweaver-Burk plot of inverse of velocities (1/V) versus inverse of substrate concentration 1/ [S] $mM^{-1}$. The Enzyme Inhibition dissociation constant *K*i was determined by secondary plot of 1/V versus inhibitor concentration. The results were processed by using SoftMaxPro.

*4.2.1.3. Free radical scavenging assay*. Radical scavenging activity was determined by modifying already reported method [47,48] by 2, 2-diphenyl-1 picrylhydrazyl (DPPH) assay. The assay solution consisted of 100 μL of DPPH (150 μM), 20 μL of increasing concentration of test compounds and the volume was adjusted to 200 μL in each well with methanol. The reaction mixture was then incubated for 30 min at room temperature. Ascorbic acid (Vitamin C) was used as a reference inhibitor. The assay measurements were carried out by using a microplate reader (OPTI $_{Max}$, Tunable) at 517 nm. The reaction rates were compared and the percent inhibition caused by the presence of tested inhibitors was calculated. Each concentration was analyzed in three independent experiments.

#### 4.2.2. In silico analysis: Computational Methodology:

*4.2.2.1. Retrieval of porcine pancreatic elastase structure*. The crystal structure of porcine pancreatic elastase was accessed from Protein Data Bank (PDB) (www.rcsb.org) with PDBID 7EST. The retrieved target protein structure was minimized by using UCSF Chimera 1.6rc [49]. The stereo-chemical properties of elastase and Ramachandran plot were also accessed from PDB [51].

*4.2.2.2. Chemo-informatics properties of synthesized compounds and molecular docking*. The synthesized compounds were evaluated on the basis of chemo-informatics properties [37–41,49–52]. Molinspiration (http://www.molinspiration.com/), and Molsoft (http://www.molsoft.com/) online servers were used to predict the chemo-informatics and biological properties of ligands, respectively. Lipinski's rule of five was analyzed using Molsoft. Before docking experiment all the synthesized chemical structures (**4a-4j**) were sketched in ACD/ChemSketch tool and accessed in mol format. Furthermore, UCSF Chimera 1.10.1 tool was employed to energy minimization of each ligand separately having default parameters such as steepest descent steps 100 with step size 0.02 (Å), conjugate gradient steps 100 with step size 0.02 (Å) and update interval was fixed at 10. Finally, Gasteiger charges were added using Dock Prep in ligand structure to obtain the good structure conformation. Molecular docking experiment was performed on all the compounds, against elastase by using virtual screening tool PyRx with VINA Wizard approach [53]. The grid box parameters values in VINA search space (X = 4.6898, Y = 57.6015 and Z = -5.7255) were adjusted with default exhaustiveness value = 8 to maximize the binding conformational analysis. We have adjusted sufficient grid box size on biding pocket residues to allow the ligand to move freely in the search space. All the synthesized compounds were docked separately against target protein. In all docked complexes, the ligands conformational poses were keenly observed to obtain the best docking results. The generated docked complexes were evaluated on the basis of lowest binding energy (Kcal/mol) values and binding interaction pattern between ligands and receptor. The graphical depictions of all the docked complexes were accomplished by UCSF Chimera 1.10.1 and Discovery Studio (2.1.0), respectively.

## Acknowledgements

We are thankful to the instrumentation facilities provided by Molecular structure determination laboratory, i-CRIM, UKM. Along with this authors are grateful to Universiti kebangsan Malaysia for financial assistance in NMR and LCMS analysis under research grant no. GUP-2019-039.

**Conflict of interest**

Authors declare no conflict of interest.

## Appendix A. Supplementary data

Supplementary data to this article can be found online at https://doi.org/10.1016/j.bioorg.2020.103906.

## References:

[1] (a) P. Lidström, J. Tierney, B. Wathey, J. Westman, Microwave assisted organic synthesis - a review, Tetrahedron 57 (2001) 9225–9283;
(b) C. Cabrele, O. Reiser, The Modern Face of Synthetic Heterocyclic Chemistry, J. Org. Chem. 81 (2016) 10109–10125;
(c) A.P. Taylor, R.P. Robinson, Y.M. Fobian, D.C. Blakemore, L.H. Jones, O. Fadeyi, Modern advances in heterocyclic chemistry in drug discovery, Org. Biomol. Chem. 14 (2016) 6611–6637.
[2] (a) M.I.M. Lazim, I.S. Ismail, K. Shaari, J.A. Latip, N.A. Al-Mekhlafi, H. Morita,

Chrotacumines E and F, Two New Chromone-Alkaloid Analogs from Dysoxylum acutangulum (Meliaceae) Leaves, Chem. Biodiverse. 10 (2013) 1589–1596; (b) M. Costa, T.A. Dias, A. Brito, F. Proença, Biological importance of structurally diversified chromenes, Eur. J. Med. Chem. 123 (2016) 487–507.
[3] S. Santhisudha, T. Sreekanth, S. Murali, B.V. Kumar, M.A. Devi, C.S. Reddy, Ultrasound Promoted Synthesis and Anticoagulant Activity of 2-Amino- 4H-chromen-4-ylphosphonates, Cardiovasc. Hematol. Agents in Med. Chem. 14 (2016) 167–174.
[4] A.M. Fouda, Synthesis of several 4H-chromene derivatives of expected antitumor activity, Med. Chem. Res. 25 (2016) 1229–1238.
[5] Z. Saffari, H. Aryapour, A. Akbarzadeh, A. Foroumadi, N. Jafari, M.F. Zarabi, A. Farhangi, In vitro antitumor evaluation of 4H-chromene-3-carbonitrile derivatives as a new series of apoptotic inducers, Tumor Biol. 35 (2014) 5845–5855.
[6] S.A. Patil, R. Patil, L.M. Pfeffer, D.D. Miller, Chromenes: potential new chemotherapeutic agents for cancer, Future Med. Chem. 5 (2013) 1647–1660.
[7] A.M. Shestopalov, Y.M. Litvinov, L.A. Rodinovskaya, O.R. Malyshev, M.N. Semenova, V.V. Semenov, Polyalkoxy Substituted 4H–Chromenes: Synthesis by Domino Reaction and Anticancer Activity, ACS Comb Sci 14 (2012) 484–490.
[8] W. O. Foye, Principi Di Chemico Farmaceutica; Piccin: Padova, Italy, (1991) 416.
[9] W. Löwe, P. von Maske, W. Müller, A khellin-like 7,7'-glycerol-bridged bischromone with anti-anaphylactic activity, Arch. Pharm. (Weinheim) 327 (1994) 255–259.
[10] C. Biot, G. Glorian, L. A. Maciejewski, J. S. Brocard, O. Domarle, G. Blampain, G. Blampain, P. Blampain, A. J. Georges, H. Abessolo, D. Dive,; J. Lebibi, Synthesis and Antimalarial Activity in Vitro and in Vivo of a New Ferrocene-Chloroquine Analogue, J. Med. Chem. 40 (1997) 3715 - 3718.
[11] M. Kidwai, S. Saxena, M.K.R. Khan, S.S. Thukral, Aqua mediated synthesis of substituted 2-amino-4*H*-chromenes and in vitro study as antibacterial agents, Bioorg. Med. Chem. Lett. 15 (2005) 4295–4298.
[12] N.J. Thumar, M.P. Patel, Synthesis and in vitro antimicrobial evaluation of 4H-pyrazolopyran, benzopyran and naphthopyran derivatives of 1*H*-pyrazole, ARKIVOC 13 (2009) 363–380.
[13] N.M. Sabry, H.M. Mohamed, E.S.A.E.H. Khattab, S.S. Motlaq, A.M. El-Agrody, Synthesis of 4H-chromene, coumarin, 12*H*-chromeno[2,3-*d*]pyrimidine derivatives and some of their antimicrobial and cytotoxicity activities, Eur. J. Med. Chem. 46 (2011) 765–772.
[14] G. Shanthi, P.T. Perumal, U. Rao, P.K. Sehgal, Synthesis and antioxidant activity of indolyl chromenes, Indian J. Chem. 48B (2009) 1319–1323.
[15] L. Bonsignore, G. Loy, D. Secci, A. Calignano, Synthesis and pharmacological activity of 2-oxo-(2*H*) 1-benzopyran-3-carboxamide derivatives, Eur. J. Med. Chem. 28 (1993) 517–520.
[16] G. P. Ellis, In the Chemistry of Heterocyclic Compounds: Chromenes, Chromanes and Chromones: Weissberger, A.; Taylor, E. C. Eds.; John Wiley: New York, 120 (1977) 11.
[17] D. Armetso, W.M. Horspool, N. Martin, A. Ramos, C. Seaone, Synthesis of cyclobutenes by the novel photochemical ring contraction of 4-substituted 2-amino-3,5-dicyano-6-phenyl-4*H*-pyrans, J. Org. Chem. 54 (1989) 3069–3072.
[18] R. Pratap, V.J. Ram, Natural and Synthetic Chromenes, Fused Chromenes, and Versatility of Dihydrobenzo[*h*]chromenes in Organic Synthesis, Chem. Rev. 114 (2014) 10476–10526.
[19] A.Z. Halimehjania, N. Keshavarzi, One-pot Three-component Route for the Synthesis of Functionalized 4*H* chromenes Catalyzed by $ZrOCl_2{\cdot}8H_2O$ in Water, J. Heterocyclic Chem. 55 (2018) 522–529.
[20] B. Siedle, A. Hrenn, I. Merfort, Natural compounds as inhibitors of human neutrophil elastase, Planta Med. 73 (2007) 401–420.
[21] N. Azmi, P. Hashim, D.M. Hashim, N. Halimoon, N.M. Nik Majid, Anti-elastase, anti-tyrosinase and matrix metalloproteinase-1 inhibitory activity of earthworm extracts as potential new anti-aging agent, Asian Pac. J. Trop. Biomed. 4 (2014) 348–352.
[22] S.I.S. Rattan, L. Sodagam, Gerontomodulatory and youthpreserving effects of zeatin on human skin fibroblasts undergoing aging in vitro, Rejuvenation Res. 8 (2005) 46–57.
[23] D.W. Kim, I. Hwang, D.W. Kim, K.Y. Yoo, C.K. Won, W.K. Moon, M.H. Won, Coenzyme Q10 effects on manganese superoxide dismutase and glutathione peroxidase in the hairless mouse skin induced by ultraviolet b irradiation, Bio. Factors 30 (2007) 139–147.
[24] M. Berneburg, H. Plattenberg, K. Medve-Konig, A. Pfahlberg, H. Gers-Barlag, O. Gefeller, J. Krutmann, Induction of the photoaging-associated mitochondrial common deletion in vivo in normal human skin, J. Invest. Dermatol. 122 (2004) 1277–1283.
[25] M. Yaar, M.S. Eller, B.A. Gilchrest, Fifty years of skin aging, J. Investig. Dermatol. Symp. Proc. 7 (2002) 51–58.
[26] (a) T. Lafarga, M. Hayes, Bioactive peptides from meat muscle and by-products: generation, functionality and application as functional ingredients, Meat Sci. 98 (2014) 227–239; (b) Y. Sun, F. Ding, Z. Chen, R. Zhang, C. Li, Y. Xu, Y. Zhang, R. Ni, X. Li, G. Yang, Y. Sun, P.J. Stang, Melanin-dot–mediated delivery of metallacycle for NIR-II/photoacoustic dual-modal imaging-guided chemo-photothermal synergistic therapy, PNAS 116 (2019) 16729–16735.
[27] (a) I. Chiocchio, M. Mandrone, C. Sanna, A. Maxia, M. Tacchini, F. Poli, Screening of a hundred plant extracts as tyrosinase and elastase inhibitors, two enzymatic targets of cosmetic interest, Ind. Crops Prod. 122 (2018) 498–505; (b) L. Tu, Y. Xu, Q. Ouyang, X. Li, Y. Sun, Recent advances on small-molecule fluorophores with emission beyond 1000 nm for better molecular imaging in vivo, Chin. Chem. Lett. 30 (2019) 1731–1737.
[28] R. Zhang, Y. Xu, Y. Zhang, H.S. Kim, A. Sharma, J. Gao, G. Yang, J.S. Kim, Y. Sun, Rational design of a multifunctional molecular dye for dual-modal NIR-II/photoacoustic imaging and photothermal therapy, Chem. Sci. 10 (2019) 8348–8353.
[29] (a) X. Lu, Y. Zhan, Q. Ouyang, S. Bai, H. Chen, Y. Yu, Y. Zheng, Y. Sun, H. Li, Fabrication of a Tyrosine-Responsive Liquid Quantum Dots Based Biosensor through Host-Guest Chemistry, Anal. Chem. 91 (2019) 13285–13289; (b) M. Kumud, N. Sanju, In-vitro evaluation of antioxidant, anti-elastase, anti-collagenase, anti-hyaluronidase activities of safranal and determination of its sun protection factor in skin photoaging, Bioorg. Chem. 77 (2018) 159–167; (c) F. Ding, Z. Chen, W.Y. Kim, A. Sharma, C. Li, Q. Ouyang, H. Zhu, G. Yang, Y. Sun, J.S. Kim, A nano-cocktail of an NIR-II emissive fluorophore and organoplatinum(II) metallacycle for efficient cancer imaging and therapy, Chem. Sci. 10 (2019) 7023–7028.
[30] B. Hasdemir, O. Sacan, H. Yasa, H.B. Kucuk, A.S. Yusufoglu, R. Yanardag, Synthesis and elastase inhibition activities of novel aryl, substituted aryl, and heteroaryl oxime ester derivatives, Arch. Pharm. Chem. Life Sci. 351 (2018) 1700269.
[31] N. Onul, O. Ertik, N. Mermer, R. Yanardag, Synthesis and biological evaluation of Ssubstituted perhalo-2-nitrobuta-1,3-dienes as novel xanthine oxidase, tyrosinase, elastase, and neuraminidase inhibitors, J. Chem. (2018) 4386031.
[32] L. Crocetti, G. Bartolucci, A. Cilibrizzi, M.P. Giovannoni, G. Guerrini, A. Iacovone, M. Menicatti, I.A. Schepetkin, A.I. Khlebnikov, M.T. Quinn, C. Vergelli, Synthesis and analytical characterization of new thiazole-2-(3*H*)-ones as human neutrophil elastase (HNE) inhibitors, Chem. Cent. J. 11 (2017) 127.
[33] N.C. Dige, P.G. Mahajan, D.M. Pore, Serendipitous formation of novel class of dichromenopyrano pyrimidinone derivatives possessing anti-tubercular activity against M. tuberculosis $H_{37}Rv$, Med. Chem. Res. 27 (2018) 224–233.
[34] N.C. Dige, P.G. Mahajan, R.K. Dhokale, S.M. Chinchkar, M.V. Patil, D.M. Pore, Novel Route for the Synthesis of 5-(4-Hydroxy-2-oxo-2*H*-chromen-3-yl)-1,3-dimethyl-1*H*-chromeno[2,3-*d*]pyrimidine-2,4(3*H*,5*H*)-diones, Org. Prep. Proced. Int. 51 (2019) 553–565.
[35] (a) N.C. Dige, P.G. Mahajan, H. Raza, M. Hassan, B.D. Vanjare, H. Hong, K.H. Lee, J. latip, S.Y. Seo, Ultrasound mediated efficient synthesis of new 4-oxoquinazolin-3(4H)-yl) furan-2-carboxamides as potent tyrosinase inhibitors: Mechanistic approach through chemoinformatics and molecular docking studies, Bioorg. Chem. 92 (2019) 103201; (b) A.R.S. Butt, M.A. Abbasi, A. Rehman, S.Z. Siddiqui, M. Hassan, H. Raza, S.A.A. Shah, S.Y. Seo, Synthesis and structure-activity relationship of elastase inhibiting novel ethylated thiazole-triazole acetamide hybrids: Mechanistic insights through kinetics and computational contemplations, Bioorg. Chem. 86 (2019) 197–209.
[36] (a) S.H. Lee, S. Sancheti, S. Sancheti, S.Y. Seo, Potent Antielastase and Antityrosinase Activities of Astilbe chinensis, Am. J. Pharmacol. Toxicol. 4 (2009) 127–129; (b) P.G. Mahajan, N.C. Dige, B.D. Vanjare, H. Raza, M. Hassan, S.Y. Seo, C.H. Kim, K.H. Lee, Facile synthesis of new quinazolinone benzamides as potent tyrosinase inhibitors: Comparative spectroscopic and molecular docking studies, J. Mol. Struct. 1198 (2019) 126915.
[37] A.K. Ghose, T. Herbertz, R.L. Hudkins, B.D. Dorsey, J.P. Mallamo, Knowledge-Based, Central Nervous System (CNS) Lead Selection and Lead Optimization for CNS Drug Discovery, ACS Chem. Neurosci. 3 (2011) 50–68.
[38] R.U. Kadam, N. Roy, Recent Trends in Drug-Likeness Prediction: A Comprehensive Review of *In Silico* Methods, Indian J. Pharm. Sci. 69 (2007) 609–615.
[39] M.A. Bakht, M.S. Yar, S.G. Abdel-Hamid, S.I. Al Qasoumi, A. Samad, Molecular properties prediction, synthesis and antimicrobial activity of some newer oxadiazole derivatives, Eur. J. med. Chem. 45 (2010) 5862–5869.
[40] S. Tian, J. Wang, Y. Li, D. Li, L. Xu, T. Hou, The application of *in silico* drug-likeness predictions in pharmaceutical research, Adv. drug deliv. Rev. 86 (2015) 2–10.
[41] M.P. Giovannoni, I.A. Schepetkin, L. Crocetti, G. Ciciani, A. Cilibrizzi, G. Guerrini, A.I. Khlebnikov, M.T. Quinn, C. Vergelli, Cinnoline derivatives as human neutrophil elastase inhibitors, J. Enzyme Inhib. Med. Chem. 31 (2016) 628–639.
[42] S.S. Hamdani, B.A. Khan, A. Saeed, F.A. Larik, S. Hameed, P.A. Channar, K. Ahmad, E.U. Mughal, Q. Abbas, N.U. Amin, S.A. Ghumro, H. Maitlo, M. Hassan, H. Raza, S.Y. Seo, Densely substituted piperidines as a new class of elastase inhibitors: Synthesis and molecular modeling studies, Arch. Pharm. (Weinheim). 352 (2019) 1900061.
[43] J.A. Kraunsoe, T.D. Claridge, G. Lowe, Inhibition of human leukocyte and porcine pancreatic elastase by homologues of bovine pancreatic trypsin inhibitor, Biochemistry 35 (1996) 9090–9096.
[44] G.D. Liyanaarachchi, J.K.R.R. Samarasekera, K.R.R. Mahanama, K.D.P. Hemalal, Tyrosinase, elastase, hyaluronidase, inhibitory and antioxidant activity of Sri Lankan medicinal plants for novel cosmeceuticals, Ind. Crops Prod. 111 (2018) 597–605.
[45] A. Saeed, D. Shahzad, F.A. Larik, P.A. Channar, H. Mahfooz, Q. Abbas, M. Hassan, H. Raza, S.Y. Seo, G. Shabir, Synthesis of 4-aryl-2, 6-dimethyl-3, 5-bis-N-(aryl)-carbamoyl-1, 4-dihydropyridines as novel skin protecting and anti-aging agents. Bangladesh, J. Pharmacol. 12 (2017) 210–215.
[46] A.R.S. Butt, M.A. Abbasi, S.Z. Siddiqui, M. Hassan, H. Raza, S.A.A. Shah, S.Y. Seo, Synthesis and structure-activity relationship of elastase inhibiting novel ethylated thiazole-triazole acetamide hybrids: Mechanistic insights through kinetics and computational contemplations, Bioorg. Chem. 86 (2019) 197–209.
[47] (a) C. V. K. Reddy, D. Sreeramulu, M. Raghunath, Antioxidant activity of fresh and dry fruits commonly consumed in India. Food Res. Inter. 43(2010) 285–288; (b) A. S. Kamarozamana, N. Ahmata, S. N. M. Isa, Z. Z. Hafiz, M. I. Adenan, M. I. M. Yusof, N. F. N. Azmin, J. Latip, New dihydrostilbenes from Macaranga heynei I.M. Johnson, biological activities and structure-activity relationship, Phytochemistry Lett. 30 (2019) 174–180.
[48] A. Saeed, P.A. Mahesar, P.A. Channar, F.A. Larik, Q. Abbas, M. Hassan, H. Raza,

S.Y. Seo, Hybrid pharmacophoric approach in the design and synthesis of coumarin linked pyrazolinyl as urease inhibitors, kinetic mechanism and molecular docking, Chem. Biodivers. 14 (2017) e1700035.
[49] E.F. Pettersen, T.D. Goddard, C.C. Huang, G.S. Couch, D.M. Greenblatt, E.C. Meng, T.E. Ferrin, UCSF Chimera–a visualization system for exploratory research and analysis, J. Comput. Chem. 25 (2004) 1605–1612.
[50] V.B. Chen, W.B. Arendall, J.J. Headd, D.A. Keedy, R.M. Immormino, G.J. Kapral, L.W. Murray, J.S. Richardson, D.C. Richardson, MolProbity: all-atom structure validation for macromolecular crystallography, Acta Crystallogr D Biol Crystallogr 66 (2010) 12–21.
[51] D. Studio, Discovery. "version 2.1." Accelrys: San Diego, CA (2008).
[52] S. Dallakyan, A. J. Olson, Small-molecule library screening by docking with PyRx. Methods, Mol. Biol. 1263(2015) 243-250.
[53] P. Ertl, B. Rohde, P. Selzer, Fast Calculation of Molecular Polar Surface Area as a Sum of Fragment-Based Contributions and Its Application to the Prediction of Drug Transport Properties, J. Med. Chem. 43 (2000) 3714–3717.